Spectroscopic applications of the (p,π^-) reaction

Z-J. Cao,* R. D. Bent, H. Nann, and T. E. Ward†
Indiana University Cyclotron Facility, Indiana University, Bloomington, Indiana 47405
(Received 9 October 1986)

Using the strong selectivity of the $A(p,\pi^-)A+1$ reaction for population of high-spin, two-particle one-hole final states, we have located and identified several candidates for high-spin states in the *sd*-shell nuclei ^{20}Na, ^{24}Al, ^{26}Si, ^{28}P, ^{30}S, and ^{31}S. The spin assignments are based on both the strong population of the states and the stretched-state signature of the analyzing power angular distributions.

I. INTRODUCTION

The purpose of most (p,π) experiments performed at the Indiana University Cyclotron Facility (IUCF) and other intermediate-energy nuclear physics laboratories during the past several years has been to elucidate the reaction mechanism. This task has proved to be a difficult one that is unlikely to be fulfilled in the near future. In this paper, we bypass the reaction mechanism problem and simply use the (p,π^-) reaction as a spectroscopic tool, in the absence of a complete understanding of the reaction dynamics. This is possible because of the striking selectivity of the (p,π^-) reaction for high-spin, two-particle one-hole final states with respect to the target ground-state configuration, which has been observed for a number of targets in the C, Ca, and Zr mass regions[1,2] and two targets in the *sd* shell.[3] This selectivity results from the large momentum transfer involved in the process together with the dominance of a specific two-nucleon reaction mechanism.[1,2] Thus, the (p,π^-) reaction may be useful in identifying high-spin states having a simple 2p-1h configuration with respect to the target nucleus, which may not be easily reached or identified by other means.

For the ^{18}O$(p,\pi^-)^{19}$Ne reaction,[3] the strongest peak in the spectrum occurs at about 4.7 MeV excitation energy, corresponding to a known $13/2^+$ state in ^{19}Ne. No states are known at 10.0 MeV excitation energy where another strong peak is seen in the spectrum, however, a $13/2^+$ state is known at 10.42 MeV in the mirror nucleus ^{19}F. Recent shell-model calculations of Wildenthal and co-workers[4] predict the first two $13/2^+$ states in the $A=19$ system to be at 4.79 and 9.89 MeV, in good agreement with the two strong peaks in the ^{18}O$(p,\pi^-)^{19}$Ne spectrum. There are two strong peaks in the ^{26}Mg$(p,\pi^-)^{27}$Si spectrum[3] corresponding to 7.0 MeV and 9.5 MeV excitation energies in ^{27}Si. The only independent evidence for high-spin assignments to these states comes from the recent shell-model calculations of Wildenthal and co-workers,[4] which predict the first $13/2^+$ state at 6.75 MeV and several high-spin states in the neighborhood of 9.5 MeV excitation energy in the $A=27$ system.

The qualitative correspondence between some of the main features of the ^{18}O$(p,\pi^-)^{19}$Ne and ^{26}Mg$(p,\pi^-)^{27}$Si spectra[3] and the full *sd*-shell model calculations[4] suggest that the (p,π^-) reaction may provide useful spectroscopic information about other *sd*-shell nuclei. Accordingly, we have measured (p,π^-) spectra for several targets in the *sd* shell, ^{19}F, ^{23}Na, ^{25}Mg, ^{27}Al, ^{29}Si, and ^{30}Si, to locate possible high-spin states. For two cases, ^{19}F$(p,\pi^-)^{20}$Na and ^{27}Al$(p,\pi^-)^{28}$P, both differential cross section and analyzing power angular distributions were measured, lending additional support for our conjectures.

II. EXPERIMENTS

The (p,π^-) experiments described in this paper were performed using 199.6 MeV proton beams from IUCF. The energy spread of the beams was about 200 keV at a beam intensity of 200 nA.

Pions were detected using the IUCF quadrupole-quadrupole split-dipole (QQSP) pion spectrograph, which has been described in detail elsewhere.[3,5,6] The focal plane detection system consists of a vertical drift chamber[7] (VDC) followed by three plastic scintillators. The VDC is used to measure both position and angle of the particle rays. From this information the position of a virtual focal plane is calculated, thus removing the optical aberrations associated with the spectrometer. The scintillators following the VDC give both energy and timing information, which are used for particle identification and background reduction.

The self-supporting targets for this experiment included ^{7}Li ^{19}F, ^{23}Na, ^{25}Mg, ^{27}Al, ^{29}Si, and ^{30}SiO$_2$. The thickness of all the targets was chosen to be 50–60 mg/cm^2, so that the energy spread in the target was less than 100 keV, to be compatible with the energy spread in the proton beams.

Pions from the most likely target contaminants, ^{12}C and ^{16}O, are kinematically well separated from the pions of interest for all of the targets. The ^{7}Li in the LiF target was used for energy calibration of the ^{19}F and other spectra at high excitation energies. Three strong peaks in the ^{7}Li$(p,\pi^-)^8$B spectrum, corresponding to the ground state and the first two excited states of ^{8}B, occur in an energy region corresponding to about 15 MeV excitation energy in ^{20}Na. Therefore, a clean ^{19}F$(p,\pi^-)^{20}$Na spectrum was obtained up to about 15 MeV excitation energy.

We obtained spectra at $\theta_{lab}=30°$ for all the targets at a constant QQSP magnetic field setting using a 199.6 MeV polarized proton beam. The polarization was around 0.8 for both spin-up and spin-down beams. Angular distribu-

tions of the differential cross sections and analyzing powers were also measured for ^{19}F from 30° to 150° in the laboratory frame in 15° steps and for ^{27}Al at three angles; 30°, 90°, and 130°.

The main systematic errors in the present measurements are due to uncertainties in the thickness and uniformity of the target (±5%), the correction for pion decay in flight (±2%)[5] and the spectrograph solid angle (±10%).[5] The statistical errors depend on the number of pion and background counts.

III. ENERGY CALIBRATION

The off-line external sorting program RQSQLQ (Ref. 6) and the peak-fitting program HOPEFIT (Ref. 8) were used to analyze the data. The program HOPEFIT allows simultaneous fitting of the spin-up and spin-down spectra to reduce the error in the fitting process.

The ^{7}Li(p,π^-)^{8}B (0.78 MeV) and ^{29}Si(p,π^-)^{30}S(g.s.) peaks were used as energy calibration points in the high and low energy regions, respectively. A linear relationship between pion momentum and position in the focal plane was assumed.[5] The pion momenta and channel numbers corresponding to position in the focal plane were 110.74 MeV/c and 64.97, respectively, for the 0.78 MeV state of ^{8}B, and 135.25 MeV/c and 155.14 for the ground state of ^{30}S. Here, we have assumed the reaction to take place at the center of the target, and the pion momentum was obtained by a relativistic kinematics calculation with target thickness corrections. Then, the equation relating the pion linear momentum p to the position x is

$$p = 0.272x + 93.08 \ . \quad (1)$$

This equation was applied to the known levels, such as the ground state and the 2.32 MeV state of ^{8}B, to check its accuracy. The pion momenta for the ground and 2.32 MeV states of ^{8}B are, respectively, 112.195 MeV/c and 107.800 MeV/c from Eq. (1), and 112.118 MeV/c and 107.802 MeV/c from relativistic kinematics. The agreement is satisfactory ($\Delta p/p = 0.07\%$). We then used Eq. (1) to calculate the pion momenta for all strong peaks in the pion spectra corresponding to low excitation energies. These pion momenta together with the relativistic kinematics give the excitation energies of the levels in the residual nuclei. The results are given in Table I, where the known levels are also listed for comparison. The known levels in the nuclei of mass 24 to 31 are from Ref. 9, while the known levels in ^{20}Na are from Ref. 10.

A quadratic relation between pion momentum and position in the focal plane was also tried, again using the 0.78 MeV state of ^{8}B and the ground states of ^{30}S and ^{31}S as calibration points. This procedure indicated a negligible quadratic term, so the excitation energies given in Table I were obtained using the linear relation of Eq. (1).

The spread in values of E_x determined from spectra taken at different angles varies between 0.02 and 0.2 MeV for most of the known levels over the whole measured energy region. Consequently, the excitation energies of the levels determined from the (p,π^-) reaction are believed to be uncertain by about ±0.1 MeV. This is compatible with the systematic errors, the energy resolution of the experiment, and the error for the peak centroids given by the peak-fitting code HOPEFIT.

TABLE I. Energies of levels strongly populated in the (p,π^-) reaction and inferred spin assignments.

	Present work		Known levels	
Nucleus	E_x[a] (MeV)	J	E_x (MeV)	J
^{20}Na	0.74		0.77	≤4[b]
	1.85		1.92	≤5[b]
	3.01	6 or 7	2.89	
	4.11	6 or 7	4.33	
^{24}Al	0.03		0.00	4
	1.22		1.12	2[b]
			1.29	3[b]
	3.39		3.35	2[b]
	4.39		4.34	
			4.53	
	5.19	3–8		
^{26}Si	−0.17		0.00	0
	2.50		2.78	2
	7.08	2–8	7.15	
	8.25	2–8		
	12.00	2–8		
^{28}P	−0.04		0.00	3
			0.11	2
	1.11		1.13	3[b]
	2.32	2–7	2.10	4[b]
	3.37		3.24	
	4.73	2–7	4.94	
^{30}S	0.00		0.00	0
	2.19		2.21	2
	3.49		3.40	2
			3.68	1[b]
	5.95	4 or 5	5.90	
	7.46	4 or 5		
	9.13	4 or 5		
	10.07	4 or 5		
^{31}S	0.05		0.00	1/2
	2.20		2.24	5/2
	3.19		3.08	1/2
			3.29	5/2[b]
			8.16	
	8.33	9/2	8.36	
			8.45	
	10.58	(9/2)		
	13.33	(9/2)		

[a]Errors ≈±0.1 MeV for all excitation energies determined from the (p,π^-) reaction.
[b]The spin and parity of the corresponding isobaric analog state.

The ^{7}Li(p,π^-)^{8}B reaction was used for energy calibration of the other 30° spectra. In Figs. 1(a) and 1(b), we see clearly three sharp peaks corresponding to the well-resolved states of known spin and parity in ^{8}B, namely, the ground (2^+), 0.78 MeV (1^+), and 2.32 MeV (3^+) states. Here, the 0.78 MeV state of ^{8}B was used for ener-

gy calibration of the other spectra in the high excitation energy region. We note that these three peaks, which sit on the top of the continuum of the ^{19}F(p,π^-)^{20}Na reaction, are well separated from the low lying states of ^{20}Na due to the large difference in Q values for the two reactions.

IV. RESULTS AND DISCUSSION

The spectra corresponding to excitation energies from zero up to about 20 MeV are shown in Fig. 1. These spectra were all taken at a laboratory angle of 30° and a bombarding energy of 199.6 MeV, without changing the QQSP magnetic field to facilitate accurate cross energy calibrations, as described above. Angular distributions of the differential cross sections and analyzing powers for several of the strongest transitions for the ^{19}F and ^{27}Al targets are presented in Figs. 2–4. These contain some useful spectroscopic information and will be discussed below.

The energy resolution obtained from the full width at half maximum of well-resolved peaks is about 150 keV for all of the spectra. This resolution is determined mainly by the beam energy spread and the target thickness.

Four strong peaks are observed in the ^{19}F(p,π^-)^{20}Na spectrum shown in Fig. 1(b), corresponding to excited states of ^{20}Na at 0.74, 1.85, 3.01, and 4.11 MeV. We see no ground-state (2^+) transition, probably due to the low spin of this state. All four peaks are broader than the instrumental resolution, indicating that more than one state contributes to each peak. There are several levels in ^{20}Na around 0.77 MeV with $J^\pi \leq 4^+$. Levels of known energy but unknown spin are at 1.92, 2.89, and 4.33 MeV. Several levels with $J \leq 5$ are known around 1.92 MeV in the isobaric analog nucleus ^{20}F. Our data are consistent with the known energy levels of ^{20}Na.

The strong populations and analyzing power patterns can be used to make tentative spin assignments to certain levels in ^{20}Na. The transitions can be grouped into two categories according to distinctly different patterns of the analyzing power angular distributions. The first group includes transitions to the 0.74 and 1.85 MeV states. The shapes of their analyzing power angular distributions, as shown in Fig. 2, are similar to those observed by Throwe[6] for transitions to low-spin final states. The second group includes transitions to the 3.01 and 4.11 MeV states. Their analyzing power angular distributions, as shown in Fig. 3, are similar to those observed for transitions to stretched two-particle one-hole states in near-threshold (p,π^-) studies on several targets from A=19 to A=89.[3,6] This type of analyzing power angular distribution seems to be a "signature" of (p,π^-) transitions to stretched two-particle one-hole final states, and is distinctly different from the type illustrated by Fig. 2. The possible final-state spins resulting from a stretched 2p-1h configuration with respect to the target nucleus, $[(\pi d_{5/2})^2_4(\nu d_{5/2})^{-1}]_{13/2^+}$ or $\{[(\pi d_{5/2})(\pi d_{3/2})]_4(\nu d_{5/2})^{-1}\}_{13/2^+}$, coupled to the $1/2^+$ target ground state, are $J^\pi=6^+$ and 7^+, assuming that all active nucleons are restricted to the *sd* shell, which is reasonable for low lying excited states. Consequently, the 0.74 and 1.85 MeV states have $J \leq 5$. This agrees with existing knowledge of the level structure of ^{20}Na and the shell model calculations of Wildenthal,[4] which predict a 5^+ level at 1.74 MeV but no higher spin levels in this excitation region. The 3.01 and 4.11 MeV states may be assigned $J^\pi=6^+$ or 7^+, based on the above analyzing power signature argument. These may correspond to the lowest 6^+ and 7^+ states predicted by Wildenthal[4] at 4.52 and 4.46 MeV, respectively. The spins of these states are not known from other experiments. A high-spin assignment explains why a strong 4.11 MeV peak is seen in the spectrum in a region where the ^{20}Na level density is high.

Figure 1(c) shows the ^{23}Na(p,π^-)^{24}Al spectrum. The peak at 1.22 MeV excitation energy is broader than the experimental resolution, indicating more than one contributing state. Two states are known around 1.22 MeV, one at 1.12 MeV and another at 1.29 MeV, which cannot be resolved completely in our experiment. The 3.39 and 4.39 MeV peaks may also represent unresolved states. The strongest peak in the spectrum corresponds to an excitation energy of 5.19 MeV. There is no known level in ^{24}Al at this excitation energy, but a number of levels are known around this energy in the isobaric analog nucleus ^{24}Na. The strong population of the 5.19 MeV state in the (p,π^-) reaction implies a possible high-spin, two-particle one-hole $[3 \leq J \leq 8]$ configuration, $[(\pi d_{5/2})^2_4(\nu d_{5/2})^{-1}]_{13/2^+} \times 3/2^+$, $\{[(\pi d_{5/2})(\pi d_{3/2})]_4(\nu d_{5/2})^{-1}\}_{13/2^+} \times 3/2^+$, or $[(\pi d_{3/2})^2_2(\nu d_{5/2})^{-1}]_{9/2^+} \times 3/2^+$, for this state. This may correspond to the second 6^+ and/or first 7^+ state(s) predicted[4] at 5.29 and 5.31 MeV, respectively. The first 8^+ state is predicted[4] at 8.29 MeV. This may correspond to one of the prominent peaks observed in the (p,π^-) spectrum at 7.65 and 8.90 MeV; however, a number of high-spin ($J=7,8$) states are predicted[4] in this energy region.

The ^{29}Si(p,π^-)^{30}S spectrum is shown in Fig. 1(d). The ground state of ^{30}S (0^+) is weakly populated but well separated from the first excited state, so it was used as a calibration point in the low energy region, as described above. The strongest three peaks in the low energy region correspond to excitation energies of 2.19, 3.49, and 5.95 MeV. These agree with known energy levels. The 5.95 MeV peak may correspond to the 5.90 MeV state identified from the (p,t) two-nucleon pickup reaction at 40 MeV;[11] a 5.95 MeV state (4^+) is known in the isobaric analog nucleus ^{30}Si. Peaks in the (p,π^-) spectrum are observed at higher excitation energies of 7.46, 9.13, 10.07, 11.53, and 13.28 MeV. The possible spin values resulting from the stretched two-particle one-hole configuration $[(d_{3/2})^2(d_{5/2})^{-1}]_{9/2^+}$ coupled to the $1/2^+$ target ground state are $J^\pi=4^+$ and 5^+. Wildenthal[4] predicts a 4^+ state at 5.91 MeV, which may correspond to the strong 5.95 MeV peak in the (p,π^-) spectrum. The lowest lying 5^+ states are predicted[4] at 7.24, 8.94, and 10.0 MeV, in close agreement with the 7.46, 9.13, and 10.07 peaks in the (p,π^-) spectrum.

There are no striking peaks in the ^{25}Mg(p,π^-)^{26}Si spectrum shown in Fig. 1(e). The low lying states are weakly populated. The 7.08 MeV peak may correspond to a known state at 7.15 MeV. Two sharp peaks at 8.25 and

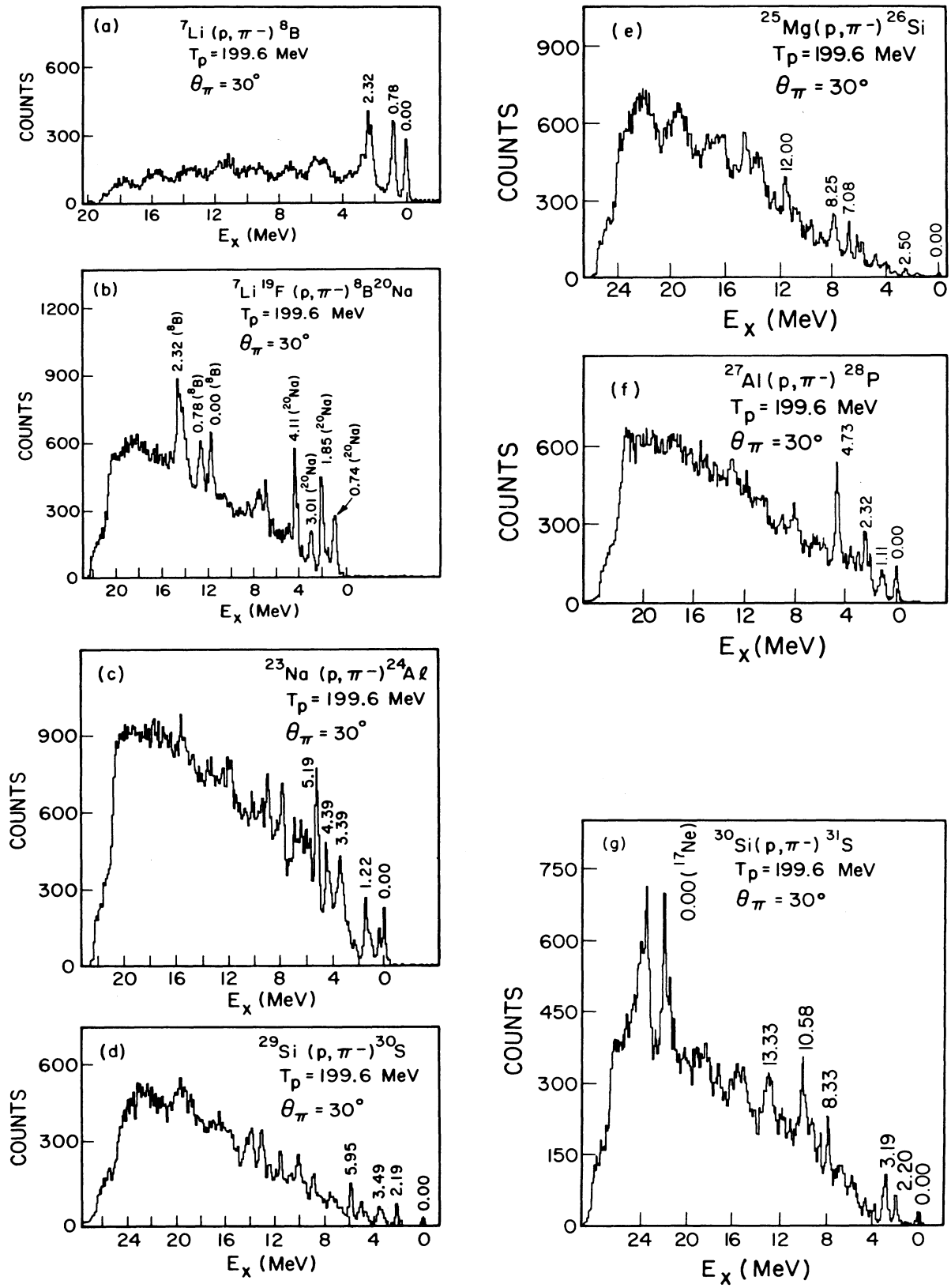

FIG. 1. Spectra from the reactions ^{7}Li(p,π^-)^{8}B (a); ^{7}Li ^{19}F(p,π^-)^{8}B ^{20}Na (b); ^{23}Na(p,π^-)^{24}Al (c); ^{29}Si(p,π^-)^{30}S (d); ^{25}Mg(p,π^-)^{26}Si (e); ^{27}Al(p,π^-)^{28}P (f); and ^{30}Si(p,π^-)^{31}S (g); at $T_p = 199.6$ MeV and $\theta_\pi = 30°$. The strong peaks seen in the high excitation energy region in (g) are due to oxygen in the target.

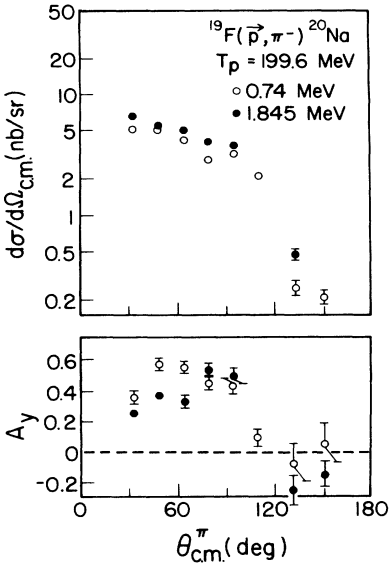

FIG. 2. Comparison of the angular distributions of the cross sections and analyzing powers for transitions to the 0.74 and 1.85 MeV states in the ^{19}F(p,π^-)^{20}Na reaction at 199.6 MeV bombarding energy, showing a striking similarity between the distributions.

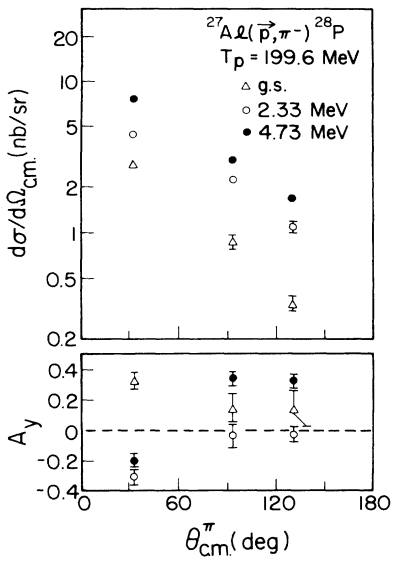

FIG. 4. The angular distributions of the cross sections and analyzing powers for the ground, 2.33 MeV, and 4.73 MeV state transitions in the ^{27}Al(p,π^-)^{28}P reaction at a bombarding energy of 199.6 MeV.

12.0 MeV excitation energies, where the level density is high, are candidates for high-spin $[2 \leq J \leq 8]$ states resulting from the stretched 2p-1h configurations $\{[(\pi d_{5/2})(\pi d_{3/2})]_4(\nu d_{5/2})^{-1}\}_{13/2^+}$ or

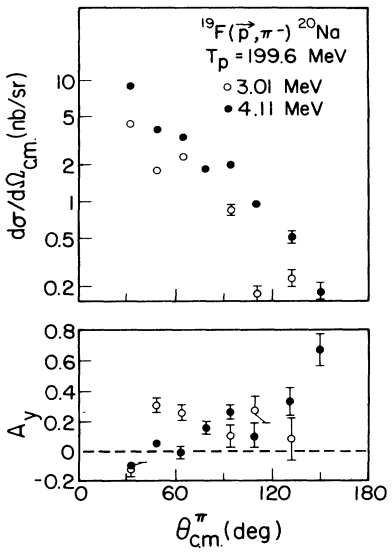

FIG. 3. Comparison of the angular distributions of the cross sections and analyzing powers for transitions to the 3.01 and 4.11 MeV states in the ^{19}F(p,π^-)^{20}Na reaction at 199.6 MeV, showing some similarity between these distributions.

$[(\pi d_{3/2})^2_2(\nu d_{5/2})^{-1}]_{9/2^+}$ coupled to the $5/2^+$ target ground state. These may correspond to the lowest energy 5^+, 6^+, and 8^+ states predicted by Wildenthal[4] at 7.04, 8.19, and 11.77 MeV, respectively.

The ^{27}Al(p,π^-)^{28}P reaction is expected to most strongly populate high-spin final states consisting of a stretched 2p-1h configuration $[(\pi d_{3/2})^2(\nu d_{5/2})^{-1}]_{9/2^+}$ coupled to the $5/2^+$ target ground state, giving $2 \leq J_f \leq 7$. The strongest peak in the spectrum shown in Fig. 1(f) occurs at $E_x = 4.73$ MeV. The angular distribution of the analyzing power for the transition to this state shown in Fig. 4 does indeed follow the systematic pattern observed[3,6] for transitions to stretched 2p-1h final states. This pattern is quite different from that observed[6] for transitions to low-spin final states, such as the ground state (3^+) transition shown in Fig. 4. The angular distribution of the analyzing power for the transition to the 2.33 MeV state is similar to that for the 4.73 MeV state suggesting a stretched 2p-1h configuration for this state also. Based on the above evidence, we tentatively associate the 4.73 MeV peak in the (p,π^-) spectrum with the 4.53 MeV (6^+) or 4.77 MeV (5^+) states predicted by Wildenthal[4] and the 2.33 MeV peak with the predicted 2.23 MeV (4^+) state. There are no spin assignments in the literature for these two states, but an analog 4^+ state is known at 2.27 MeV in ^{28}Al. We note that there are several other predicted[4] high-spin states at 2.65 MeV (5^+), 3.51 MeV (4^+), 4.29 MeV (5^+), 4.53 MeV (6^+), 5.26 MeV (5^+), and higher energies that do not show up prominently in the (p,π^-) spectrum.

We see a weak ground state transition in the ^{30}Si(p,π^-)^{31}S spectrum shown in Fig. 1(g). This is due to

the low spin ($1/2^+$) of the ground state. This peak is well separated from the second excited state peak at 2.24 MeV ($5/2^+$). The first excited state ($3/2^+$) is missing from the spectrum. Our energy calibration scheme gives energies of 0.05 and 2.20 MeV for the ground and 2.24 MeV states, respectively, showing consistency within the measurement error. The 3.19 MeV peak in the spectrum is a doublet corresponding to the known 3.08 ($1/2^+$) and 3.29 ($5/2^+$) MeV states. The 8.33 MeV peak may correspond to one of the known states at 8.18, 8.36, and 8.45 MeV, which have been identified using the ^{29}Si(^{3}He,n)^{31}S and ^{29}Si(^{3}He,nγ)^{31}S transfer reactions at 6.5 MeV.[12] The strong peaks located near the high excitation energy end of the spectrum are due to the ground state and low lying excited states of ^{17}Ne resulting from the ^{16}O(p,π^-)^{17}Ne reaction, which has a much more negative Q value than the ^{30}Si(p,π^-)^{31}S reaction. The ^{30}Si(p,π^-)^{31}S reaction is expected to populate most strongly final states containing a large component of the stretched 2p-1h configuration $[(\pi d_{3/2})^2_2(\nu d_{5/2})^{-1}]_{9/2^+}$. A $9/2^+$ state is predicted[4] at 8.31 MeV, which may correspond to the 8.33 MeV peak in the (p,π^-) spectrum; however, we note that thirteen $9/2^+$ states are predicted in the 5.21—9.0 MeV excitation energy region. The 10.58 and 13.33 MeV peaks in the (p,π^-) spectrum may correspond to states outside of the *sd*-shell model space. The results and conclusions discussed above are summarized in Table I.

V. SUMMARY AND CONCLUSIONS

We have used the (p,π^-) reaction as a spectroscopic tool to identify a number of possible high-spin, two-particle one-hole states in several *sd*-shell nuclei. These identifications are based on the systematic selectivity of the (p,π^-) reaction for high-spin 2p-1h final states that has been observed across the entire periodic table, as well as the systematic behavior of the analyzing power angular distributions observed for (p,π^-) transitions to stretched final states.[1,3,6,13] Spectra were measured at $T_p = 199.6$ MeV and $\theta_\pi = 30°$ for all cases, and angular distributions of the differential cross sections and analyzing powers were obtained in addition for the ^{19}F(p,π^-)^{20}Na and ^{27}Al(p,π^-)^{28}P reactions. Based on these measurements, a number of tentative spin assignments were made, which are summarized in Table I. Many of these assignments are consistent with recent shell model predictions[4] for the energies of high-spin states. More stringent tests of the shell model calculations require knowledge of the matrix elements of the appropriate operators between the states of interest. Independent experimental confirmations of the spin assignments inferred from the present work are also needed.

This research was supported by the National Science Foundation under Grant No. NSF PHY 84-12177.

*Present address: Physics Department, Carnegie-Mellon University, Pittsburgh, PA 15213.

†Present address: Department of Nuclear Energy, Brookhaven National Laboratory, Upton, NY 11973.

[1] S. E. Vigdor, T. G. Throwe, M. C. Green, W. W. Jacobs, R. D. Bent, J. J. Kehayias, W. K. Pitts, and T. E. Ward, Phys. Rev. Lett. **49**, 1314 (1982); Nucl. Phys. **A396**, 61c (1983).

[2] W. W. Jacobs, T. G. Throwe, S. E. Vigdor, M. C. Green, J. R. Hall, H. O. Meyer, and W. K. Pitts, Phys. Rev. Lett. **49**, 855 (1982).

[3] J. J. Kehayias, R. D. Bent, M. C. Green, M. Hugi, H. Nann, and T. E. Ward, Phys. Rev. C **33**, 1388 (1986).

[4] B. H. Wildenthal (private communication).

[5] M. C. Green, Ph.D. thesis, Indiana University, 1983 (unpublished).

[6] T. G. Throwe, Ph.D. thesis, Indiana University, 1985 (unpublished).

[7] W. Bertozzi, M. V. Hynes, C. P. Sargeny, C. Creswell, P. C. Dunn, A. Hirsch, M. Leitch, B. Norum, F. N. Rad, and T. Sasanuma, Nucl. Instrum. Methods **141**, 457 (1977).

[8] Indiana University Cyclotron Facility Internal Report, 1984.

[9] P. M. Endt and C. van der Leun, Nucl. Phys. **A310**, 96 (1978).

[10] F. Ajzenberg-Selove, Nucl. Phys. **A392**, 124 (1983); **A392**, 181 (1983).

[11] R. A. Paddock, Phys. Rev. C **5**, 485 (1972).

[12] J. M. Davidson, D. A. Hutcheon, D. R. Gill, T. Taylor, D. M. Sheppard, and W. C. Olsen, Nucl. Phys. **A240**, 253 (1975).

[13] W. W. Jacobs, in *Nuclear Structure at High Spin, Excitation, and Momentum,* Proceedings of the Workshop on Nuclear Structure at High Spin, Excitation, and Momentum Transfer held at the McCormick's Creek State Park, Bloomington, Indiana, 1985, AIP Conf. Proc. No. 142, edited by Hermann Nann (AIP, New York, 1986), p. 181.